Fast And Simple Automatic 3D Ultrasound Probe Calibration Based On 3D Printed Phantom And An Untracked Marker

Jun Shen, Nabil Zemiti, Jean-Louis Dillenseger, Philippe Poignet

Fast and Simple Automatic 3D Ultrasound Probe Calibration Based on 3D Printed Phantom and an Untracked Marker

Jun Shen[1,2], Nabil Zemiti[1], Jean-Louis Dillenseger[2] and Philippe Poignet[1]

***Abstract*— Tracking the pose of an ultrasound (US) probe is essential for an intraoperative US-based navigation system. The tracking requires mounting a marker on the US probe and calibrating the probe. The goal of the US probe calibration is to determine the rigid transformation between the coordinate system (CS) of the image and the CS of the marker mounted on the probe. We present a fast and automatic calibration method based on a 3D printed phantom and an untracked marker for three-dimensional (3D) US probe calibration. To simplify the conventional calibration procedures using and tracking at least two markers, we used only one marker and did not track it in the whole calibration process. Our automatic calibration method is fast, simple and does not require any experience from the user. The performance of our calibration method was evaluated by point reconstruction tests. The root mean square (RMS) of the point reconstruction errors was 1.39 mm.**

I. INTRODUCTION

Ultrasound (US) imaging is a safe, non-ionizing, low cost and portable medical imaging modality. Three-dimensional (3D) imaging can generate a 3D US volume of the region of interest (ROI) which provides more information about the anatomical structures than 2D US imaging. There are two kinds of 3D US imaging techniques commonly being used by clinicians. The first one is called freehand 3D US system [1] and uses a marker mounted on a 2D US probe. When the probe sweeps over the ROI, the acquired slices are stacked to reconstruct a 3D volume according to their corresponding locations in the space. However, the disadvantages of using freehand 3D US system are that it is time-consuming and does not provide real-time US volume acquisition, which is required for many intraoperative applications. In order to solve these problems, the second imaging technique generates a 3D US volume by using a dedicated 3D probe. For instance, the 2D matrix array transducer is able to perform volumetric imaging in real-time and the swept motor transducer acquires a 3D volume in 1 to 4 seconds.

Tracking the pose of the ultrasound probe is required for many intraoperative applications. However, tracking systems generally only record the pose of a marker (rigidly mounted on the US probe) with respect to a fixed coordinate system (CS). Therefore, it is essential to calibrate the pose of the US image with respect to this marker. The process of determining the rigid transformation between the CS of the US image and the CS of the marker (mounted on the probe) is called US probe calibration [2]. Common calibration approaches are based on calibration phantoms with known geometry. These phantoms can be points [3][4], wires [5][6] or planes [6][7]. The calibration problem of freehand 3D US system has been studied extensively, referring to the reviews of many published techniques [2][8]. However, the calibration procedure for calibrating freehand 3D US systems is different from calibrating 3D US probes. This is due to the fact that freehand 3D US system calibration uses points or 2D features extracted from US slices, while 3D US probe calibration uses volumetric features extracted from a 3D volume. In this study, we focus on 3D US probe calibration techniques.

Bergmeir et al. presented in [9] a calibration method based on a tracked phantom. This method achieved a higher accuracy than another method performing US imaging around an untracked fixed phantom and registering the US volumes to each other, as in hand-eye calibration. Some works directly used the tip of a tracked stylus as an imaging feature for the probe calibration [10]. However, the tracked stylus had to be calibrated before using it, and the stylus calibration introduced non-negligible errors, as reported in [11]. Some other works used planar phantoms and the phantoms' positions had to be determined in a fixed CS by a tracked calibrated stylus [12]-[14]. Their methods suffer not only from the stylus calibration errors, but also from phantom calibration errors. The use of tracked wire phantoms, as proposed in [9] and [10], includes challenges in manufacturing the wires precisely, ensuring they are straight, and correctly positioning them in water. Unlike the above calibration techniques using 3D US volumes, a study presented in [14] performed calibration on multiple slices before the 3D scan conversion process. Then, they found the best-fit path through the multiple slices calibrations and used it as the final calibration solution for a swept motor 3D probe. Although, they achieved a high calibration accuracy, their calibration procedure seems time-consuming for multiple US slices. In addition, it seems difficult to implement this method for calibrating 2D matrix array transducers which perform volumetric imaging by electronic scanning.

To the best of our knowledge, all the 3D US probe calibration methods proposed in the literature need tracking

**This work was supported in part by the French ANR within the Investissements d'Avenir Program (Labex CAMI, ANR-11-LABX0004, Labex NUMEV, ANR-10-LABX-20, and the Equipex ROBOTEX, ANR-10-EQPX-44-01), the ARC Foundation and the Région Bretagne, France.

[1]Jun Shen, Nabil Zemiti and Philippe Poignet are with the Laboratory of LIRMM, University of Montpellier, CNRS, Montpellier, France. Email: Jun.Shen@lirmm.fr, Nabil.Zemiti@lirmm.fr, poignet@lirmm.fr

[2]Jun Shen and Jean-Louis Dillenseger are with INSERM UMR 1099, Rennes, France; Universiy of Rennes 1, LTSI, Rennes, France. Email: jun.shen@univ-rennes1.fr, jean-louis.dillenseger@univ-rennes1.fr

systems to track at least two markers: the first one is rigidly mounted on the US probe, and the second one is fixed to the calibration phantom. Indeed, some of the methods need to track a third marker (attached on a stylus) for the phantom calibration to find the relationship between the features and the marker of the phantom. Since using and tracking more markers may introduce more uncertainties, we propose to use only one marker and not to track it during the calibration procedure, so that decreases the source of measurement uncertainties. This also avoids errors due to stylus calibration and phantom calibration steps.

In this study, a fast and automatic calibration method based on a 3D printed phantom and an untracked marker is proposed for 3D US probe calibration. The calibration solution is easily found by a rigid registration between the phantom's computer-aided design (CAD) model and the phantom's US image. This is because the marker's CAD model was used during the design of the phantom's CAD model, so that the position of the phantom is known in the marker's CS. The proposed automatic method is easy to implement and does not require any experience from the user. In addition, our method not only works for calibrating swept motor 3D probes, but also for calibrating 2D matrix array transducers.

II. Method

Fig.1 shows all the CSs and transformations used in a conventional US calibration procedure. As we can see, a tracking system has two mobile parts (marker n1 and n2) and a stationary counterpart (an optical pose-tracking system). Usually, the stationary part of the tracking system is defined as world coordinate system (WCS) w, and the markers' CSs and CAD models are provided by the manufacturer. The first marker n1 is rigidly fixed on the probe and its CS is represented by m. The second marker n2 is mounted on the phantom and the phantom calibration is required to relate the CS of the phantom to the CS of the marker n2. As classically presented in the literature, the CS p refers to the CS of the marker n2 after phantom calibration.

The goal of the calibration is to determine the rigid transformation ${}^{m}\mathbf{T}_{i}$ between the CS of the 3D US image i and the CS of the marker n1 m. In Fig.1, the conventional mathematical calibration framework can be presented as

$$ {}^{m}\mathbf{T}_{i} = {}^{w}\mathbf{T}_{m}^{-1}\ {}^{w}\mathbf{T}_{p}\ {}^{p}\mathbf{T}_{i} \tag{1} $$

where ${}^{b}\mathbf{T}_{a}$ is the transformation from the CS a to CS b, and i, m, p and w represent the CS of the 3D US image, the marker n1 mounted on the probe, the marker n2 attached to the phantom, the world, respectively. Therefore, to obtain the calibration solution ${}^{m}\mathbf{T}_{i}$, the main issues below have to be solved:

1) Phantom calibration: using a calibrated stylus to determine the phantom position in the CS of the marker n2 and thus in WCS, so that ${}^{w}\mathbf{T}_{p}$ is measured.
2) Registration of the phantom's US image and the phantom's geometries, so that ${}^{p}\mathbf{T}_{i}$ is obtained.
3) Tracking of the markers n1 and n2 computing the transformations ${}^{w}\mathbf{T}_{m}^{-1}$ and ${}^{w}\mathbf{T}_{p}$.

In order to simplify this calibration procedure, we propose a method based on a custom-made phantom, in which solving only problem 2) is enough to find the calibration solution. As shown in Fig.2, a marker is assembled and secured on the probe. There is no tracking of the marker needed in the whole calibration process, so we call this marker 'untracked marker'. The phantom is mounted on the untracked marker and its position is known in this marker's CS. This is due to that the marker's CAD model was used during the design of the phantom, and their CSs m and p was coincided with each other. Thus, the conventional mathematical calibration framework of Eq.1 can be simplified to

$$ {}^{m}\mathbf{T}_{i} = {}^{p}\mathbf{T}_{i} \tag{2} $$

Therefore, solving a series of problems in the conventional calibration procedure becomes solving only the registration problem between the mesh model generated from the US image and the phantom's CAD model. There is no tracking of the marker needed in our method.

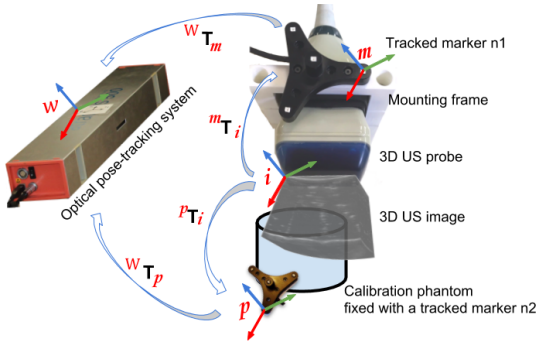

Fig. 1. Coordinate systems and transformations used in conventional calibration method: tracking system tracks the marker n1 and n2.

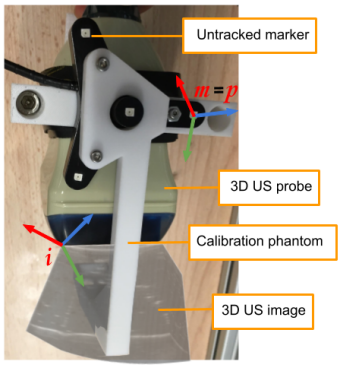

Fig. 2. Coordinate systems used in our calibration method: the calibration phantom CS p is the same as the untracked marker CS m.

A. Calibration Phantom

The calibration phantom was created as shown in Fig.3(a). At one end (right part of the Fig.3(a)), it has geometric features for US imaging. Fig.3(b) shows the axial view of this

part which consists of a box shape ($25 \times 20 \times 10$ mm^3) and 4 holes with dimensions of $\varnothing = 8$ mm, $\varnothing = 6$ mm, $\varnothing = 4$ mm and $\varnothing = 4$ mm, respectively. These features were experimentally chosen in consideration of the US probe's field of view and the quality of the acquired image. The other end of the phantom (left part of the Fig.3(a)) was designed to be attached to the marker. As shown in Fig.4, the hole in the middle of the phantom perfectly fits the protrusion of the marker, and the protrusion of $p3$ can be perfectly embedded into $p3'$. $p1$ and $p1'$, $p2$ and $p2'$ having the same diameter were fixed together by two screws. After attaching the phantom to the marker, the CS p in Fig.4 is the same as the CS m.

A 3D modeling software *SketchUp* (*Trimble Inc.*) was used to create the CAD model of our calibration phantom, and the designed model was 3D printed by the *Stratasys Fortus 400mc* prototyping machine with Polycarbonates material. The printing resolution was 0.178 mm. The CAD model of the phantom can be shared upon request. The marker used in this study was the *Boomerang* active marker from *Atracsys* with RMS calibration error of 0.04 mm. The phantom was designed to adapt to this marker, but it can adapt to other markers' CAD model.

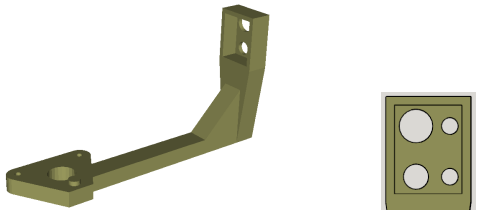

(a) (b)

Fig. 3. (a) CAD model of the calibration phantom; (b) Axial view of the phantom features used for US imaging.

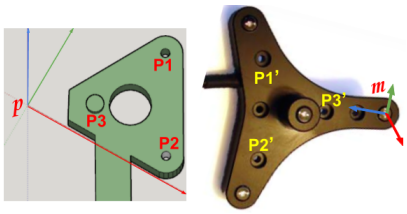

Fig. 4. Phantom's CAD model designed to be attached on the marker. CS $p = m$ in the design.

B. Data Acquisition

Before performing 3D US imaging on the calibration phantom, the phantom, the untracked marker and the probe must be assembled together, as shown in Fig.2. The marker was rigidly mounted on the probe by a 3D printed mounting frame, then, the phantom was mounted on this marker, as explained in Fig.4. The US data acquisition was simply done by placing the calibration setup into water (Fig.5(a)).

In this study, the 3D US image was acquired by a *SonixTouch Q+* ultrasound machine (*BK Ultrasound, powered by Analogic Corporation*), equipped with the *4DL14-5/38 Linear 4D* US probe. The ultrasound machine performed an US acquisition on the phantom at a transmit frequency of 10 MHz and a depth of 75 mm. These parameters were chosen to be compatible with our clinical application for tongue base surgery, but they can be adjusted for other applications. Fig.5(b) shows the sagittal and axial views of the acquired 3D US image.

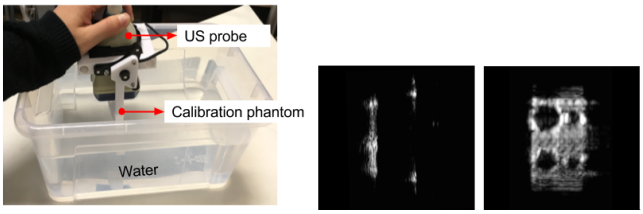

(a) (b)

Fig. 5. (a) Performing US acquisition on the calibration phantom; (b) Sagittal (left) and axial (right) view of the acquired 3D US image.

C. US to Phantom's CAD model Registration

The goal of the calibration process is to determine the rigid transformation between the CS of the 3D US image and the CS of the marker which is mounted on the probe. As shown in Eq.2, our calibration solution is found by solving only the rigid registration problem between two mesh models from the US image and the phantom. As presented in Fig.6, the olive green model was the CAD model of the phantom, and the orange mesh model was generated from an automatic segmentation of the US volume. The registration between these two 3D mesh models was accomplished by using 3D Slicer [15] surface registration. It took few seconds to compute this transformation.

The automatic segmentation was achieved by computing the directional gradients of the 3D US image and then applying Standard Hough Transform (SHT)[16] on the gradients image. Thus, 5 horizontal lines and 5 vertical lines on the plane having 4 circles were detected. The US image was automatically segmented based on the position information of these lines segments in the US image and the known geometry of the phantom.

After completing the calibration process, the phantom was removed by unscrewing it from the marker. Meanwhile, there was no relative movement between the marker and the probe, because the marker was mounted and secured on the probe by a mounting frame.

III. Results

A. Feature Exaction Accuracy

In order to evaluate the registration performed in subsection II-C, we used the target registration error (TRE) [17] which computes the distance, after registration, between corresponding points. First, landmarks were manually placed on the inner corners of the box and the centers of the circles in the 3D US image. Then, these landmarks and the corresponding features in the phantom's CAD model were

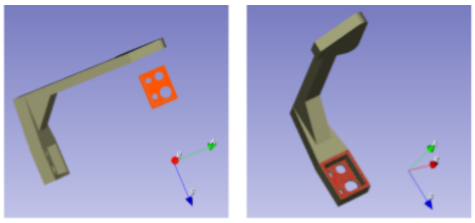

Fig. 6. CAD mesh model of the phantom (olive green) and mesh model from US segmentation (orange) before (left) and after (right) registration.

used for the TRE computation. The root mean square of the target registration error (RmsTRE) was computed to evaluate the registration performance.

We used 10 US volumes from different acquisitions and automatically segmented them. Then, the registration was performed on each of the mesh models from the automatic segmentation and the phantom's CAD model generating 10 transformations $({}^{m}\mathbf{T}_i)_{1...10}$. These transformations were used to compute the $\text{RmsTRE}_{1...10}$. The mean of the RmsTREs was $0.361\ \text{mm}$ and the standard deviation was $0.156\ \text{mm}$. The calibration procedure (including assembling calibration setup, US acquisition, automatic segmentation and mesh model registration) took 3 to 5 minutes. The user does not need to be trained.

We found that our automatic method and the manual method gave similar $\text{RmsTRE}_{1...10}$ values. A non-specialist was asked to manually segment the US volumes over several days. Then the registration was performed between each of the mesh models from the manual segmentation and the phantom's CAD model. Then, 10 transformations $({}^{m}\mathbf{T}_i)_{1...10}$ were obtained and used to compute the $\text{RmsTRE}_{1...10}$. The mean of the RmsTREs was $0.344\ \text{mm}$ and the standard deviation was $0.079\ \text{mm}$, which was slightly better than the values obtained by our automatic method. However, manual segmentation was time consuming and user-dependent. As shown in Fig.7, the RmsTRE values from automatic method have bigger variance than the values from manual method. This is because the automatic method is more sensitive to the image quality than the manual method. The US image quality can be improved by adjusting imaging parameters during the data acquisition.

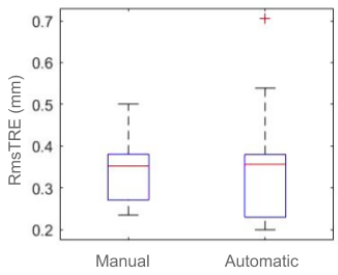

Fig. 7. RmsTRE values obtained by manual method and automatic method during registration evaluation. The smaller RmsTRE means better registration performance.

B. Point Reconstruction Accuracy

Calibration accuracy refers to how close the transformation ${}^{m}\mathbf{T}_i$ obtained from the calibration method is to the real transformation between the probe and the US volume. We used point reconstruction tests, as presented in [14], to evaluate our calibration method. The tests calculate the distance between a point (stylus tip) with a known location in the WCS w and this point transformed from US volume to the WCS w using our calibration solution. A tracked stylus was then used for the point reconstruction tests. The stylus is custom-made and consists of a marker at one end and a sharp tip at the other end. The point position of the sharp tip was obtained by a stylus calibration [18] with an error of $0.83\ \text{mm}$.

We placed the stylus tip into water and the calibrated 3D probe was used to image the tip. 20 US volumes were acquired. Both the stylus and the probe were moved between each acquisition, meanwhile, their positions were recorded by the tracking system (WCS). The tip in US volume was manually located. The point reconstruction error was calculated by

$$e = \|{}^{w}\mathbf{s} - {}^{w}\mathbf{T}_m\,{}^{m}\widehat{\mathbf{T}}_i\,{}^{i}\mathbf{s}\| \tag{3}$$

where ${}^{w}\mathbf{s}$ represents the coordinate of stylus tip in the WCS, ${}^{i}\mathbf{s}$ represents the coordinate of the stylus tip in the US image, ${}^{m}\widehat{\mathbf{T}}_i$ represents our calibration solution and ${}^{w}\mathbf{T}_m$ is the transformation between the marker CS m and the stationary part of the tracking system (WCS).

In the point reconstruction tests, we used the *Atracsys easyTrack 500* tracking system ($0.2\ \text{mm}$ RMS error at $1\ \text{m}$ distance) with the *Boomerang* active marker ($0.04\ \text{mm}$ RMS calibration error). The stylus was 3D printed and its calibration error was $0.83\ \text{mm}$. The root mean square (RMS) of point reconstruction errors was $1.39\ \text{mm}$, mean of the point reconstruction errors was $1.26\ \text{mm}$ and standard deviation was $0.62\ \text{mm}$.

IV. Discussion

As a part of an intraoperative application, a 3D US probe must be calibrated and localized in a fast and simple way with high accuracy. Our calibration procedure takes less than 5 minutes, which is much faster than the method (taking 20 minutes) presented in the study of [13].

The stylus used in the point reconstruction tests provides points with a known localization for validating our calibration method. However, the stylus is prone to errors and its pointer calibration normally has RMS errors in the range of $[0.6\ \text{mm}, 0.9\ \text{mm}]$, and as hight as $1.5\ \text{mm}$ [11]. In our study, the stylus calibration had an RMS error of $0.83\ \text{mm}$. This might introduce some errors into the point reconstruction accuracy, which may be improved with a better calibrated stylus.

The comparison of the calibration performance between our method and previous studies is difficult, due to the differences of experimental setup, protocol and environment. Furthermore, different studies use different definitions of

point reconstruction accuracy to evaluate their methods. Some well known studies reported their results using RMS or mean of point reconstruction errors. For instance, Bergmeir et al. used a cross-wire phantom and compared hand-eye calibration (HE) and typical tracked phantom method (TP). They reported mean errors of $3.5\,\mathrm{mm}$ (HE) and $3.3\,\mathrm{mm}$ (TP) [9]. Poon and Rohling compared methods based on an IXI-shaped wires phantom, a cube phantom and a stylus, and found RMS point reconstruction errors of $2.15\,\mathrm{mm}$, $4.91\,\mathrm{mm}$ and $2.36\,\mathrm{mm}$, respectively [10]. Compared to above methods, we achieved smaller RMS and mean of point reconstruction errors of $1.39\,\mathrm{mm}$ and $1.26\,\mathrm{mm}$, respectively. In [14], they proposed performing calibration on multiple 2D slices, instead of a 3D volume. Then, they found the best-fit path through the multiple slices calibrations and used it as the calibration solution for a swept motor 3D probe. They achieved an RMS point reconstruction errors of $0.93\,\mathrm{mm}$. The stylus used in their point reconstruction tests had a high accuracy which was computed by averaging the standard deviations of stylus location at 30 points achieving a value of $0.11\,\mathrm{mm}$. However, our stylus was made in our laboratory and calibrated by sphere fit method with an accuracy of $0.83\,\mathrm{mm}$. Our RMS point reconstruction accuracy will likely be improved by using a more accurate stylus in point reconstruction tests. Baumann et al. reported their method achieving an RMS point reconstruction error of $0.9\,\mathrm{mm}$, however, instead of using a stylus, they used a bead phantom made of crossed wires in their point reconstruction tests [13]. Therefore, as explained, it is very difficult to compare the performance among different methods, since they used different evaluation methods.

Besides the calibration precision discussed above, conventional calibration approaches use and track two markers: one is mounted on the probe and the other is attached to the calibration phantom. In addition, some techniques have introduced a third tracked marker (mounted on a stylus) for the phantom calibration [10][12][13][14]. Since using and tracking more markers may introduce more uncertainties into the calibration precision, we propose not to track any markers during the calibration procedure. Indeed, in conventional calibration approaches, multiple steps are prepared for the probe calibration (phantom calibration, stylus calibration, ...), which increase the calibration process duration. In our study, only one untracked marker was needed and mounted on the probe. The idea of assembling the phantom on this untracked marker, so that they share the same CS, makes the calibration procedure simple, fast and easy to implement. The fully automatic calibration method can be performed by a non-specialist. The whole calibration procedure (including assembling calibration setup, US acquisition, automatic segmentation and mesh model registration) takes less than 5 minutes.

V. CONCLUSION

A simple and efficient approach is presented for calibrating 3D US probes including 2D matrix array transducers or swept motor 3D probes. The idea of assembling the phantom, the untracked marker and the probe together greatly simplifies the conventional calibration procedures. The fully automatic calibration method does not require any experience or skills from the user. Future work will improve the stylus used in the validation process.

REFERENCES

[1] Gee, A., Prager, R., Treece, G. and Berman, L.: Engineering a freehand 3D ultrasound system. Pattern Recognition Letters, 24(4), 757-777 (2003).

[2] Mercier, L., Langø, T., Lindseth, F. and Collins, L.D.: A review of calibration techniques for freehand 3-D ultrasound systems. Ultrasound in Medicine & Biology, 31(2), 143-165 (2005).

[3] Detmer, P.R., Bashein, G., Hodges, T., Beach, K.W., Filer, E.P., Burns, D.H. and Strandness, D.E.: 3D ultrasonic image feature localization based on magnetic scanhead tracking: in vitro calibration and validation. Ultrasound in Medicine & Biology, 20(9), 923-936 (1994).

[4] Trobaugh, J.W., Richard, W.D., Smith, K.R. and Bucholz, R.D.: Frameless stereotactic ultrasonography: method and applications. Computerized Medical Imaging and Graphics, 18(4), 235-246, (1994).

[5] Carr, J.: Surface reconstruction in 3D medical imaging. Ph.D. Thesis, University of Canterbury, Christchurch, New Zealand (1996).

[6] Prager, R.W., Rohling, R.N., Gee, A.H. and Berman, L.: Rapid calibration for 3-D freehand ultrasound. Ultrasound in Medicine & Biology, 24(6), 855-869 (1998).

[7] Rousseau, F., Hellier, P., and Barillot, C. Confhusius: A robust and fully automatic calibration method for 3D freehand ultrasound. Medical Image Analysis, 9(1), 25-38 (2005).

[8] Hsu, P.W., Prager, R.W., Gee, A.H. and Treece, G.M.: Freehand 3D ultrasound calibration: a review. Advanced Imaging in Biology and Medicine, 47-84 (2009).

[9] Bergmeir, C., Seitel, M., Frank, C., De Simone, R., Meinzer, H.P. and Wolf, I.: Comparing calibration approaches for 3D ultrasound probes. International Journal of Computer Assisted Radiology and Surgery, 4(2), 203 (2009).

[10] Poon, T.C. and Rohling, R.N.: Comparison of calibration methods for spatial tracking of a 3-D ultrasound probe. Ultrasound in Medicine & Biology, 31(8), 1095-1108 (2005).

[11] Hsu, P.W., Prager, R.W., Houghton, N.E., Gee, A.H. and Treece, G.M.: Accurate fiducial location for freehand 3D ultrasound calibration. Medical Imaging: Ultrasonic Imaging and Signal Processing, 6513, 651315 (2007). International Society for Optics and Photonics (2007).

[12] Lange, T., Kraft, S., Eulenstein, S., Lamecker, H. and Schlag, P.M.: Automatic calibration of 3D ultrasound probes. In Bildverarbeitung für die Medizin, 169-173 (2011).

[13] Baumann, M., Daanen, V., Leroy, A. and Troccaz, J.: 3-D ultrasound probe calibration for computer-guided diagnosis and therapy. International Workshop on Computer Vision Approaches to Medical Image Analysis, 248-259 (2006).

[14] Abeysekera, J.M., Najafi, M., Rohling, R. and Salcudean, S.E.: Calibration for position tracking of swept motor 3-d ultrasound. Ultrasound in Medicine and Biology, 40(6), 1356-1371 (2014).

[15] Fedorov A., Beichel R., Kalpathy-Cramer J., Finet J., Fillion-Robin J.C., Pujol S., Bauer C., Jennings D., Fennessy F., Sonka M., Buatti J., Aylward S.R., Miller J.V., Pieper S. and Kikinis R.: 3D Slicer as an image computing platform for the quantitative imaging network. Magnetic Resonance Imaging, 30(9), 1323-41 (2012).

[16] Gerig, G. and Fernand K.: Fast contour identification through efficient Hough transform and simplified interpretation strategy. In Proceedings-International Conference on Pattern Recognition. IEEE (1986).

[17] Fitzpatrick, J.M., West, J.B. and Maurer, C.R.: Predicting error in rigid-body point-based registration. IEEE Transactions on Medical Imaging, 17(5), 694-702 (1998).

[18] Leotta, D.F., Detmer, P.R. and Martin, R.W.: Performance of a miniature magnetic position sensor for three-dimensional ultrasound imaging. Ultrasound in Medicine and Biology, 23(4), 597-609 (1997).